Journal of Applied Polymer Science

Development and Characterization of Composite Chitosan/Active Carbon Hydrogels for a Medical Application

Pochat-Bohatier Céline,[1] Venault Antoine,[2] Bouyer Denis,[1] Vachoud Laurent,[3] David Laurent,[4] Faur Catherine[1]

[1]IEM (Institut Europeen des Membranes), UMR 5635 (CNRS-ENSCM-UM2), Universite Montpellier 2, Place E. Bataillon, F-34095, Montpellier, France

[2]Department of Chemical Engineering, Chung Yuan Christian University, Chung Li City, Taiwan

[3]UMR Qualisud – Laboratoire Physique moléculaire et structurale, Faculté de Pharmacie, 15 avenue C. Flahault BP 14491, 34093 Montpellier Cedex 5, France

[4]Ingénierie des Matériaux Polymères, IMP, UMR CNRS 5223, Laboratoire IMP@Lyon 1, Université Claude Bernard Lyon 1, Université de Lyon, 15 bd A. Latarjet, Bât. Polytech Lyon, 69622 Villeurbanne Cedex, France

Correspondence to: F. Catherine (E-mail: Catherine.Faur@iemm.univ-montp2.fr)

ABSTRACT: Composite chitosan/active carbon (AC) hydrogels were elaborated by a novel route, consisting in exposing the chitosan solution to ammonia vapors. This vapor-induced gelation method was compared with the conventional elaboration process, a direct immersion of the chitosan solution in liquid ammonia. The hydrogels were characterized to evaluate their potential application as wound-dressings, mostly regarding their morphology, mechanical properties, swelling behavior, and sorption capacities for malodorous compounds emitted from wounds as diethylamine (DEA). The influence of elaboration route, chitosan concentration, and AC incorporation was studied. The results show that freeze-dried hydrogels have a porous asymmetric structure dependent on the chitosan concentration and which promotes exudates drainage. The nanostructure of the parent hydrogel is semi-crystalline and slightly dependent on the gelation conditions. It confers on hydrogel an acceptable mechanical behavior (compressive modulus up to $1.08 \cdot 10^5$ Pa). Hydrogels including AC display enhanced sorption kinetics for DEA, with sorption capacities up to 49 mg g^{-1}. © 2012 Wiley Periodicals, Inc. J. Appl. Polym. Sci. 000: 000–000, 2012

KEYWORDS: biomedical applications; biopolymers and renewable polymers; composites; phase behavior; properties and characterization

Received 24 May 2012; accepted 27 July 2012; published online
DOI: 10.1002/app.38414

INTRODUCTION

Because of its exceptional biological properties (bioactive, biocompatible, and bioresorbable), chitosan can be used, in the form of hydrogels or porous scaffolds, for numerous medical applications as tissue engineering or drug delivery.[1] However, wound dressing is one of the most promising medical applications for chitosan materials, which have been shown to promote the cutaneous tissue regeneration by an enhancement of cellular proliferation.[2] Commercial dressings prepared from chitin or chitosan are mostly under dried form, films, or fibers.[3,4] Recent studies point out the fact that hydrophilic hydrogels based on (bio)-polymer materials are considered as promising options to the requirements of ideal wound dressings for the treatment of local wound infections, in terms of infection prevention, moisture environment, structure, biocompatibility, and biodegradability.[5,6] More specifically, physical hydrogels of chitosan, only constituted by chitosan and water, could be successfully applied to the treatment of full-thickness burn injuries because of their ability to promote cell proliferation, in particular, by a humidity control above the wound.[7,8]

Besides wound healing, another target of ideal wound dressings is to reduce the emission of malodorous amine-based volatile molecules (cadaverine and putrescine) produced by proteolytic bacteria during the healing process of chronic wounds. These odorous emissions represent a serious problem for the patients and the medical staff. One of the methods widely adopted to avoid such emissions is the association of an adsorbent material, active carbon (AC), with wound dressings. Yet, a few studies mention the association of AC and chitosan within a single composite but they all aimed at removing pollutants from water

combining the sorption properties of both AC and chitosan, and are thus applied in the field of water treatment and not in the medical field. To test the ability of wound dressing to remove malodorous compounds, the diethylamine (DEA) may be considered as model molecule.[9,10]

The preparation of chitosan physical hydrogels can be achieved using a neutralization process without any use of organic solvent or crosslinking additive to preserve the chitosan compatibility for biomedical applications.[11] Over the critical concentration for chain entanglements (C*), the mechanism of gelation is attributed to the formation of physical inter-chains junctions: chitosan is first dissolved in acetic acid aqueous solution to achieve the stoichiometric protonation of the $-NH_2$ sites. Then, by contacting the polymer solution to a base (ammonia), the apparent charge density of chitosan chains is decreased by a proton transfer from the amine moieties of chitosan (chit-NH_3^+) to the base (NH_3), resulting in the gel matrix formation. Two different procedures to contact the chitosan aqueous solution with a base have been reported.[7,12] The traditional method to induce gelation consists in an immersion of the polymer solution in ammonia or sodium hydroxide solution. A novel elaboration route, the "vapor gelation process," uses gaseous ammonia instead of ammonia solution, so that a progressive displacement of the interface—related to the sol–gel transition—occurs across the chitosan sample to form the physical hydrogel.

In our recent article, we investigated this novel "vapor gelation process" by a rheology study to show that some specific formulation and process parameters significantly influenced the viscoelastic properties of the gels. Increasing the chitosan concentration, the exposure time of chitosan systems to ammonia vapors and the temperature of the reactor led to an increase in the physical crosslink density of the networks and resulted in an improvement of the gel storage modulus of the hydrogels.[13] We also developed a gelation model including mass transfers and reactions assuming a Fickian diffusion and neither influence of chitosan nor AC on the water and the ammonia activities to predict the concentration profiles of ammonia and chitosan species with reaction time.[14]

The scope of this work was now to explore the influence of the gelation route, i.e., a direct immersion in ammonia solution (wet gelation process) or exposure to gaseous ammonia (vapor gelation process), on composite chitosan/AC hydrogel potential for wound dressing applications. To this aim, the obtained materials were characterized in terms of structure and swelling behavior. A second objective of this study was to prepare composite wound dressings, associating chitosan with active carbon, for the treatment of malodorous wounds. Such a strategy was intended to add a sorption functionality of malodorous compounds to the wound dressing material. Liquid phase experiments were performed to assess the sorption properties of the composite hydrogels for DEA, to simulate the contact of the dressing with the wound exudates. Moreover, structural and mechanical properties of the composite AC/chitosan hydrogels were compared with those of chitosan hydrogels, to determine the impact of active carbon powder on the morphology, and mechanical behavior of wound dressing materials.

EXPERIMENTAL

Reagents

Chitosan was supplied as flakes by France Chitine (Batch type 342 from shrimp shells). It has a viscosity of 100 cP at 25°C (data producer), a mass average molecular weight of 180,000 g mol^{-1} and a 20% degree of acetylation (producer data and Proton Magnetic Nuclear Resonance measurement deduced by the Hirai method).[15] The detailed characterization was described in a previous study.[13] The AC used in this study is a commercial powdered product from Norit (Amersfoort, The Netherlands) listed in the European pharmacopoeia. N_2 adsorption isotherm at 77 K, performed with a Micromeritics 2010 analyzer after degas for 48 h at 300°C, enabled to assess the specific surface area of AC of 1546 $m^2\ g^{-1}$ and a micropore volume of 0.932 $cm^3\ g^{-1}$.

DEA ($C_4H_{11}N$, Molecular Weight: 73.14 g mol^{-1}) was purchased from Aldrich (reagent grade), and analyzed with a Hitachi U-2001 UV–Visible spectrophotometer at a wavelength of 204 nm.

Elaboration of Chitosan and Composite Chitosan/Active Carbon Hydrogels

Preparation of the Solutions. Chitosan solutions were obtained by dissolving chitosan powder in a diluted acetic acid solution to achieve stoichiometric protonation of the amine moieties, according to the following chemical reaction:

$$\text{Chit} - NH_2 + AcOH \leftrightarrow \text{Chit} - NH_3^+ + AcO^- \qquad (1)$$

where Chit–NH_2 is the free amine form of chitosan, and AcOH is the undissociated acetic acid form. Chit–NH_3^+ is representing the protonated form of chitosan, soluble in water, and AcO^- the acetate ion.

The final chitosan concentration in solutions ranged from 3.00 to 4.00 ± 0.01% (w/v). Below 3% (w/v), the mechanical properties of the gels were not sufficient for handling the samples. For chitosan concentrations higher than 4% (w/v), the final solutions were too viscous and it was difficult to obtain a homogeneous casting. In the case of composite hydrogels, the chitosan powder was mixed with AC powder, the AC concentration being kept at a constant value of 0.13 ± 0.001% (w/v). Solutions were stirred for 24 h to ensure a complete homogenization, degassed for 12 h and then stored at 4°C until use.

Elaboration of Hydrogels Using the Wet Gelation Process. Chitosan solutions (9 ± 0.1 g), with or without AC, were poured into Petri dishes with a 5-cm inner diameter and then immersed in 100 mL of a 1-mol L^{-1} ammonia aqueous solution used as the gelation agent. After 24 h immersion duration, the obtained hydrogels were rinsed with deionized water to remove the excess of ammonia and reach neutral pH, and then stored at 4°C in deionized water.

Elaboration of Hydrogels Using the Vapor Gelation Process. In the case of the vapor-gelation process, the same chitosan solution with or without AC was poured in a Petri dish and exposed to ammonia vapors in a dedicated double-walled closed chamber (Legallais). The ammonia vapors were

previously generated from ammonia aqueous solution (1.126% w/w) placed in the chamber 1 h before the onset of the gelation experiment to reach the vapor/liquid equilibrium. Temperature was controlled to 30 ± 1°C. Therefore, the ammonia partial pressure inside the reactor was also controlled to 1680 Pa. The relative humidity ranged between 96 and 98 ± 1%. The experimental scheme was previously presented.[14] In this case, gelation was induced by the contact between the chitosan solution and the ammonia vapors produced from the thermo-regulated ammonia solution. The exposure time to the ammonia vapors was set to 12 h. This duration guaranties a complete gelation for the given operating conditions.[14] Subsequently, the obtained hydrogels were rinsed with deionized water until neutral pH and stored at 4°C in deionized water until use.

Characterization of the Chitosan and Chitosan/Active Carbon Hydrogels

Nanostructure. To characterize the nanostructure of chitosan hydrogels and study their semi-crystalline morphology before significant drying in air, small angle X-ray scattering (SAXS), and wide angle X-ray scattering (WAXS) were performed at the European Synchrotron Radiation Facility (ESRF) in Grenoble (France) at the BM2-D2AM beamline. Synchroton radiation was useful in this case to avoid the drying of samples during the experiment (less than 30 s). The data were collected at incident photon energy of 16 keV with a sample to detector distance of 160 and 14 cm for SAXS and WAXS, respectively. A bi-dimensional detector (CDD camera, Ropper Scientific) was used and data corrections were performed using the software BM2D2AM developed on the beamline. The data were corrected for dark current, flat field response, and camera distortion. Finally, silver behenate was used as a calibration standard to deduce the scattering vector values for all pixels of the images and radial averages around the beam center.

Compressive Modulus. The Young modulus (E) was extracted from uni-axial compression measurements at room temperature by a texturometer TA-XT (Stable Micro Systems). Hydrogel samples with a thickness of 1 cm were compressed at a cross-head speed of 0.6 mm min^{-1}. The Young modulus was defined as the initial linear modulus on the stress–strain curve. These measurements were performed on swollen hydrogels. The compression tests calculations performed in this study used the compression stress at 10% applied strain. The results presented were the mean value of three independent measurements.

Sorption Properties for DEA. Sorption kinetics of DEA onto chitosan hydrogels, AC powders, and chitosan-AC composites elaborated by the wet gelation process were performed in tightly sealed batch reactors to avoid any loss by volatilization. A total of 30 mg of active carbon (alone in solution or entrapped in a 4% chitosan hydrogel) was continuously stirred at 500 rpm and 25 ± 2°C in 300 mL of a 100 mg L^{-1} DEA aqueous solution. The DEA concentration in solution was determined at regular time-steps by UV spectrophotometry at 204 nm (Hitachi U2001) to plot adsorption kinetics. It was verified that there was no removal of DEA over the experiment duration when solutions did not contain active carbon. The sorption kinetic experiments were used to monitor the sorption dynamics and find out the required time to reach the equilibrium. The sorption capacity at time t (Q_t, mg g^{-1}) could then be calculated from a mass balance equation, where (C_t, mg L^{-1}) is the concentration of DEA in solution at time t, V and C_0 are the volume and the initial concentration of the DEA solution, and m is the total mass of the materials (chitosan hydrogel, AC powder, or AC/chitosan composite hydrogel):

$$Q_t = \frac{(C_0 - C_t)V}{m} \tag{2}$$

At equilibrium, eq. (2) could also be used to calculate equilibrium sorption capacity (Q_e, mg g^{-1}) from the measurement of equilibrium concentration of DEA in solution (C_e, mg L^{-1}).

Initial kinetic coefficients γ (L mg^{-1} min^{-1}) were also calculated from the initial slope of the kinetic curves $(dC/dt)_{t\to 0}$, weighted by operating conditions:

$$\gamma = \left(\frac{dC}{dt}\right)_{t\to 0}\frac{V}{mC_0} \tag{3}$$

The first-order k_I (h^{-1}, over the first 20–30 min of the sorption process) and second order k_{II} [g (mg h)$^{-1}$, over the whole sorption process] kinetic constants could also be calculated according to the Lagergren expression and the pseudo-second-order equation applied when time t tends to 0:[16,17]

$$\log(Q_e - Q_t) = \log q_e - k_I . t/2.303 \tag{4}$$

$$t/Q_t = 1/k_{II} \cdot q_e^2 + t/q_e \tag{5}$$

In both eqs. (4) and (5), q_e is the theoretical equilibrium sorption capacity calculated by the kinetic model.

Elaboration of the Chitosan and Chitosan/Active Carbon Freeze-Dried Systems

Freeze-drying of hydrogels was considered in this work with the aim of inducing a sponge-like structure which may be an ideal characteristic for cell migration, adhesion, proliferation, and which could facilitate oxygen transport.[18] It can be envisioned that such systems could be rehydrated before use.

Chitosan and composite chitosan/active carbon hydrogels were frozen at −30°C. Afterward, they were freeze dried during 24 h under 75 μbar. Despite lyophilization may alter the parent structure of the hydrogel involving behavior and structure different from that of initial hydrogels, the structures of lyophilized samples were considered as representative of the hydrogels structures in several previous works on chitosan hydrogels.[19,20] This hypothesis that could not be confirmed in this study; however, we observed the absence of significant macroscopic shrinkage (<10%) from the evolution of the gel diameters before and after freeze-drying.

Characterization of the Chitosan and Chitosan/Active Carbon Freeze-Dried Systems

Morphology in the Micron Range. For each elaboration condition, different gels were elaborated and freeze-dried using the same protocol to be observed by a Scanning Electron Microscope HITACHI S 4800.

Applied Polymer SCIENCE

Swelling Study. The swelling behavior of freeze-dried materials was studied to assess the water sorption capacity, and to examine their relative ability for exudates drainage. The rehydration of lyophilizates is also a method to obtain hydrated samples that will contribute to maintain the hydration level of the wound. The classical gravimetric method was used to determine the swelling kinetics and the equilibrium swelling ratio (ESR) of the gels. Lyophilized gels were immersed at 37°C into distilled water. The samples were taken out from water at regular time-steps. Then, water onto the rehydrated systems surfaces was gently wiped out with a wet filter paper and the sample weights were measured. This operation was repeated thrice for each sample, and the average value was taken as the weight value. The swelling kinetics was recorded measuring the weight of the swollen samples until equilibrium was reached. The ESR was then calculated from:

$$\mathrm{ESR} = \frac{W_s - W_d}{W_d} \tag{6}$$

where W_d and W_s are the weight of the lyophilized (dried) samples and the weight of the swollen sample at equilibrium, respectively.

RESULTS AND DISCUSSION

Nanostructure Characterization of Hydrogels

WAXS allowed determining the crystalline character of the hydrogels. The WAXS patterns obtained for chitosan hydrogels elaborated by the wet and the vapor gelation processes and for both chitosan contents of 3 and 4% (w/v) are presented in Figure 1(a). In the q-range below 0.4 $Å^{-1}$, the scattered intensity is due to the nano-heterogeneity of the gels; the amorphous halo due to water can be clearly observed with a maximum close to 2 $Å^{-1}$ and a high-q shoulder above 2.4 $Å^{-1}$.[21] Although the chitosan fraction did not exceed 4% (w/v) in this work, the contribution of crystallites could be evidenced by the shoulder in the q range 1.35–1.45 $Å^{-1}$. Figure 1(a) thus points out that physical hydrogels prepared in this study are semi-crystalline matrices whatever the elaboration process used. These results are not in full agreement with previous studies reporting that chitosan hydrogels mainly led to amorphous systems, since the crystallinity in highly hydrated forms is difficult to detect but easily evidenced when the polymer is under a dry form (powder, film, lyophilizate).[22] Figure 1(b) displays a close view of the diffraction diagrams normalized to the value of the maximum of the halo of water close to 2 $Å^{-1}$. As expected, the diffraction contribution of chitosan is higher for the hydrogels at the highest concentrations 4% (w/v). The wet process yields semi-crystalline hydrogels with a broader diffraction peak indicative of smaller or more defective chitosan crystallites. It was confirmed by an apparent coherent crystalline size L close to 70 Å for the immersion (wet) process and to 80 Å for the vapor gelation route (L was calculated according to the Scherrer formula : $L \sim 2\pi/\Delta q$, where Δq is the full width of the diffraction peak). Such values can be considered as lower bounds for the size of crystallites since the broadening effect of crystalline defects is not taken into account. Thus, in the investigated conditions, the elaboration process (wet or vapor gelation routes) slightly

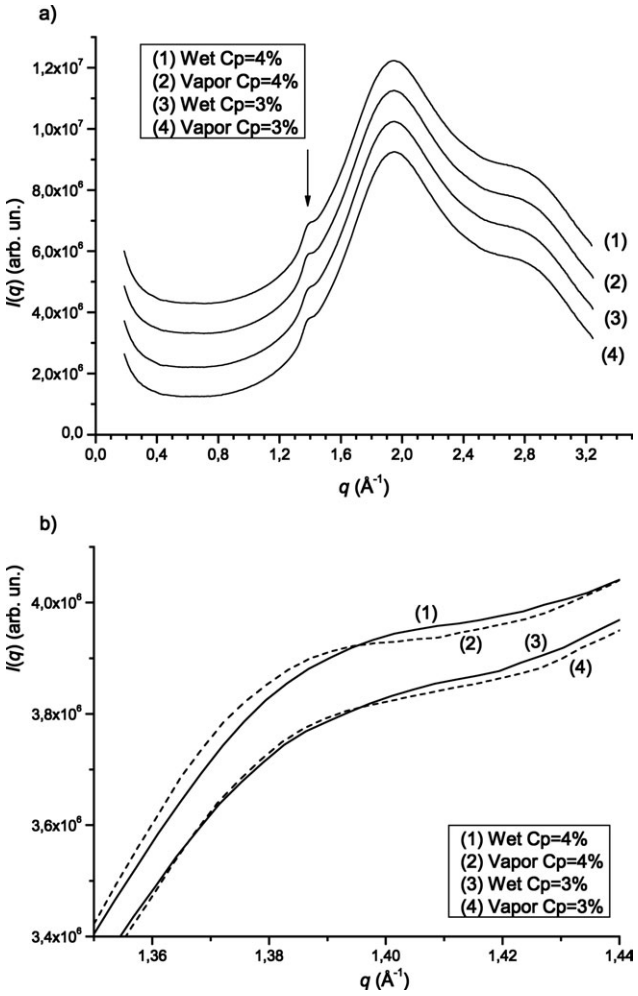

Figure 1. (a) Wide Angle X-ray Scattering diagrams of chitosan hydrogels at 3 and 4% (w/v) obtained after immersion in 1 M ammonia aqueous solution during 24 h (wet route) or after contact with ammonia vapors 12 h (vapor route). The diffraction patterns were shifted for clarity (1): $+3.10^6$ arb un. (2): $+2.10^6$ arb. un. (3): $+1.10^6$ arb. un. (b) Close view of the diffraction peak of the crystalline phase of chitosan within hydrogels.

impacted on the nanostructure of hydrogels, despite larger or less defective crystallites being obtained with the vapor gelation process.

To complete the morphology characterization in a larger size range, a SAXS study was also carried out. The scattered patterns (Figure 2) were modeled in the entire q range investigated by the general Porod's law:

$$I(q) = \frac{C}{q^{\alpha}} \tag{7}$$

where C is the generalized Porod's constant and α the Porod's exponent found to be close to 2.30 for all systems. Such a trend evidences that the heterogeneities responsible for the scattering behavior of chitosan hydrogels cannot be ascribed only to a collection of crystalline platelets with random orientation, which would correspond to a generalized Guinier law with a α value of 2.[23] Based on a recent classification of the nanostructure of

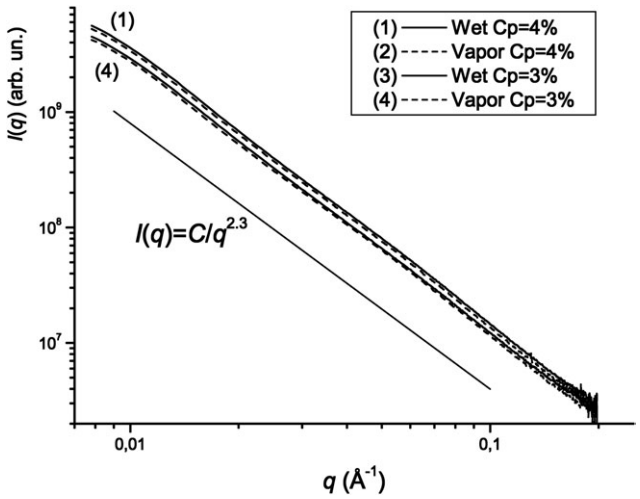

Figure 2. Small Angle X-ray Scattering diagrams of chitosan hydrogels of different concentrations, 3 and 4% (w/v), and processed according to different gelation routes: immersion in 1 *M* ammonia aqueous solution during 24 h (wet route) or after contact with ammonia vapors 12 h (vapor route).

chitosan hydrogels, this scattering behavior leading to a power law with intermediate exponent value of 2.3 may result from the crystallites in the high q range, and would be superimposed to the contribution of aggregates of various sizes and shapes in the lower q range.[24] Whatever the gelation process used to prepare the hydrogels – either wet gelation or vapor gelation route – the SAXS patterns obtained are very similar. This result permits to conclude that in the chosen neutralization conditions, there is no significant influence of the interface nature (liquid/liquid or vapor/liquid) between the polymeric solution and the alkaline compound structuring of chitosan hydrogels in the larger characteristic size range. Such similarity could in turn be due to similar neutralization kinetics as demonstrated from numerical results in a previous work.[14] The evolution of the area contribution A_{chit} of chitosan in the diffraction diagrams of hydrogels shows that the crystallinity ratio is not significantly impacted by the gelation route. The effect of chitosan concentration C_p is evidenced in Figure 2, displaying the increase of the crystalline contribution of chitosan with the polymer concentration of the chitosan hydrogels from 3 to 4 % (w/v). It can be numerically evaluated by the ratio $r = A_{chit(Cp\ =\ 4\%)}/A_{chit(Cp\ =\ 3\%)}$. Such values of "$r$" are close to 1.15 and 1.1 for the wet and vapor neutralization processes respectively, showing that the crystalline fraction of chitosan is not directly proportional to chitosan concentration. Indeed, crystallization could be limited by the entanglement density, i.e., the viscosity of the solution at the gelation step, a lower concentration favoring chain mobility and subsequent crystallization.

Morphology of Freeze-Dried Systems

The effects of the elaboration process and chitosan and AC contents on the morphology of freeze-dried hydrogels are shown in SEM photographs in Figure 3. All cross-sections in Figure 3(a–f) show that freeze-dried chitosan hydrogels are characterized by a dense skin supported by a sub-layer consisting in a highly macroporous structure, whose pores form an interconnecting "open-cell" structure. This asymmetric morphology was observed in previous studies of chitosan materials as well as hydrogels obtained by exposition to ammonia vapors or membranes elaborated by immersion in a gelation bath.[11,25] These asymmetric membranes, through the dense skin, may provide a protection barrier to the wound preventing external bacterial contamination and allow the control of the water loss from the wound. The sponge-like porous layer, with pore diameters ranging from 100 to 500 μm, may enable the drainage of wound exudates and provide space for tissue regeneration by cell colonization.[18,25] For the same chitosan content of 3% (w/v), the size of pores of the sublayer seems more important for materials elaborated by the wet process Figure 3(d) compared with those produced by the vapor gelation route Figure 3(a). This observation will be further related with swelling behavior. Moreover, the increase of the chitosan content from 3 to 4% (w/v) seems to reduce the pore size of the sublayer close to the dense skin as

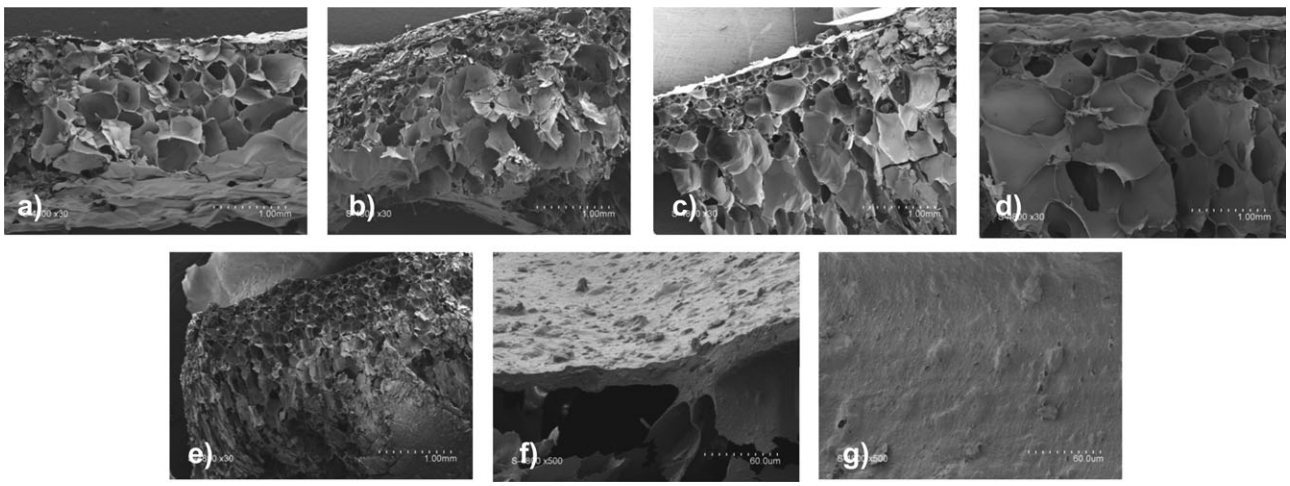

Figure 3. Scanning electron micrographs of freeze-dried chitosan hydrogels elaborated by : (a) vapor route, C_p = 3% (w/v); (b) vapor route, C_p = 3.5 % (w/v); (c) vapor route, C_p = 4 % w/v; (d) wet route, C_p = 3% (w/v). Scanning electron micrographs of freeze-dried composite chitosan/AC hydrogels elaborated by vapor route, C_p = 3 % (w/v) : (e) cross-section (f) dense skin surface (g) pore wall.

Applied Polymer SCIENCE

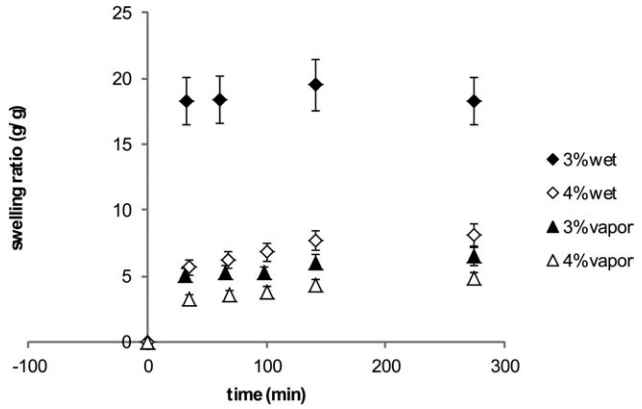

Figure 4. Effect of gelation route and chitosan content C_p on the swelling kinetics of freeze-dried chitosan hydrogels. (◆) wet route for C_p = 3% (w/v); (◇) wet route for C_p = 4 % (w/v); (▲) vapor route for C_p = 3% (w/v); (△) vapor route for C_p = 4% (w/v).

shown by Figure 3(a–c). The inclusion of AC in the chitosan hydrogels leads to a global asymmetric morphology [Figure 3(e)] quite similar to that of chitosan hydrogels elaborated in the same conditions [Figure 3(a)]. The AC nanoparticles seem to be dispersed at the surface of the dense skin [Figure 3(f)] as well as inside the chitosan matrix of the sublayer [Figure 3(g)].

Swelling Behavior

The interesting morphology of the lyophilized hydrogels led us to examine their swelling behavior in terms of kinetics and ESR in water. Figure 4 compares the swelling kinetics obtained for freeze-dried chitosan hydrogels elaborated by both gelation processes and for 3 and 4% (w/v) chitosan concentrations. It evidences a fast increase of the degree of swelling in the first 30 min of immersion reaching 90% of the value at equilibrium in this time range, followed by a slower process leading to the final equilibrium after 70 min. A similar trend for swelling kinetics was obtained for chitosan-based materials as crosslinked chitosan gel and chitosan/γ-poly(glutamic acid) polyeletrolyte complex.[26,27] Concerning the effect of elaboration conditions of the parent hydrogels, this figure emphasizes that gels are more likely to swell at lower chitosan concentration (for gels elaborated by the wet process, ESR = 19.5 g/g and 7.3 g/g for 3 and 4% chitosan respectively). This may be explained by the fact that entangled junctions between chitosan chains are less numerous at low concentration, which facilitates diffusion of water molecules inside the matrix and thus its hydration and swelling. In addition, Figure 4 highlights the better swelling of freeze-dried hydrogels elaborated by the wet process (for a 3% chitosan concentration, ESR = 19.5 and 6.5 g/g for wet and vapor gelation processes, respectively). In complement with these data on dried hydrogels, the chitosan concentrations of rehydrated lyophilizates (gels) at the swollen state (C_{ps}) may be calculated for both elaboration processes, accounting for the initial chitosan weight used to prepare the chitosan solution (W_{po}) and the weight of the swollen hydrogel at equilibrium (W_s):

$$C_{ps} = \left(1 - \frac{W_s - W_{po}}{W_s}\right) \cdot 100 \qquad (8)$$

It appears that chitosan concentrations of gels at the swollen state are lower for samples elaborated by the wet process (3.41 and 5.88% w/v for an initial concentration of 3 and 4% w/v, respectively) compared with those elaborated by contact with a vapor phase (4.42 and 11.1% w/v for an initial concentration of 3 and 4% w/v, respectively). These lower chitosan concentrations at the swollen state for wet samples are in agreement with the more opened porosity of the sponge-like sublayer observed on the freeze-dried structure [Figure 3(d)], which facilitates the sorption of water. High ESR values are in agreement with published data for chitosan-based materials as well as chitosan membranes, which typically present ESR from 1 to 9 g/g, chitosan fibers which swell from 1 to 5 g/g or carboxymethylchitosan hydrogels that were shown to have an ESR from 8 to 36 g/g.[4,25,28]

Mechanical Characterization of Hydrogels: Compressive Modulus

The evaluation of the mechanical properties of the hydrogels has been assessed using static tests by the determination of the values of uniaxial compressive modulus (E). They were determined for chitosan hydrogels and for composite hydrogels, elaborated by both processes. The results are displayed in Figure 5. The values of compressive modulus ranged from 28,300 to 107,700 Pa for chitosan hydrogels while they reached 138,400 Pa for composite materials. These values are comparable to compressive modulus obtained for crosslinked chitosan hydrogels in the swollen state or for swollen composite chitosan/γ-PGA hydrogels.[24,27]

The hydrogels elaborated by the vapor gelation process exhibit slightly improved elastic properties (especially with AC), with respect to hydrogels elaborated by the wet process, but this behavior cannot be considered as significant in all elaboration conditions.

The values of compressive modulus highlight better mechanical properties of hydrogels as the chitosan concentration increases from 3 to 4% (w/v). This improvement of mechanical properties observed for high chitosan concentrations is due to a higher density of chain segments within the interchain interaction zones. The occurrence of hydrogen bonds, hydrophobic junctions, crystallites, and entanglements inherited from the solution is therefore more important at high polymer concentration, enhancing the mechanical properties of the hydrogels.[11,29] This result is in agreement with ESR measurements and with the

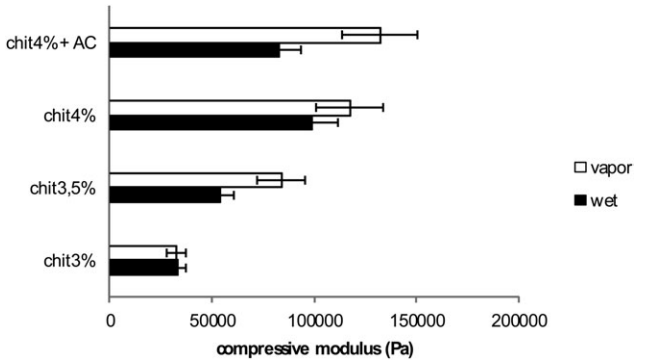

Figure 5. Effect of gelation route, chitosan content, and inclusion of AC on the compressive modulus of hydrogels elaborated by the (■) wet route; (□) vapor route.

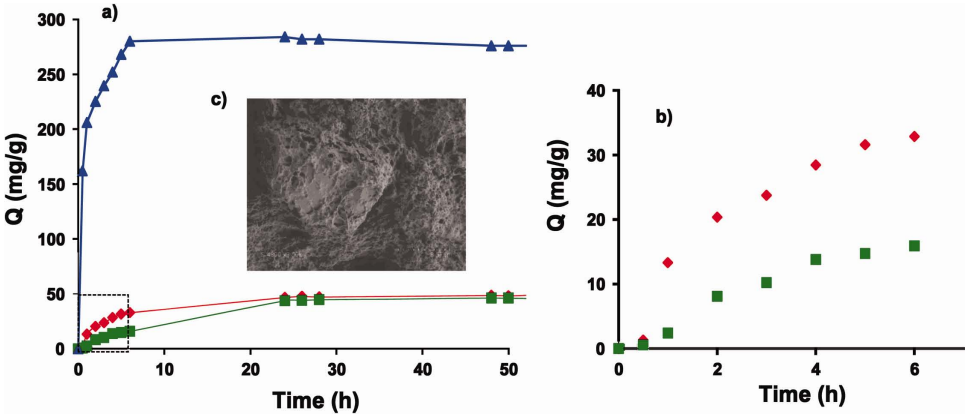

Figure 6. DEA sorption onto composite and chitosan hydrogels and onto activated carbon powder. Composite gel, Chitosane gel, activated carbon. [Color figure can be viewed in the online issue, which is available at wileyonlinelibrary.com.]

crystalline morphology of the samples deduced from synchrotron WAXS patterns.

The presence of active carbon did not permit to improve significantly the compressive modulus, despite the published reports mentions the use of active carbon to enhance the mechanical properties of polymer matrices. More specifically, the tensile strength of carboxymethylated chitosan films was increased by inclusion of AC nanoparticles.[30] However, to be fully effective, AC particles have to be homogeneously distributed in the polymer matrix to avoid the formation of AC aggregates in the gel structure. This homogenization is generally performed by an ultrasonic stirring of the composite solution. In our study, to avoid the polymer degradation by ultrasonic radiation, a magnetic stirring was performed.[31] Consequently, even though SEM images exhibited homogeneous distribution of AC particles within the polymer matrix, it was possibly not optimal and could still be improved. In addition, the low concentration of AC in chitosan hydrogel (0.13% w/v) may certainly explain the weak influence of AC on the compressive modulus values that are very close for chitosan and composite hydrogels.

Sorption Properties for Malodorous Compounds

Sorption kinetics of DEA by AC, chitosan, and chitosan/AC composite hydrogels are presented in Figure 6. The sorption behavior of composite hydrogels was compared with those obtained with the compounds alone (AC or chitosan) to figure out the role of AC in the sorption process. Chitosan hydrogel alone is already an effective material for the removal of DEA with an equilibrium capacity Q_e of about 46 mg of DEA per gram of chitosan hydrogel. However, such a removal capacity is much lower than that of AC alone, for which the equilibrium capacity was measured to be 280 mg g^{-1}, which shows the better efficiency of AC to adsorb DEA. Nevertheless, when AC was entrapped within the polymeric matrix [as seen in micrographs Figure 2(f, g) and Figure 6(c)] the sorption capacity of the composite hydrogel chitosan/AC reached only 49 mg of DEA per gram of composite materials. Considering that the composite hydrogels contains 30 mg of AC and that the resulting increase in the equilibrium sorption capacity is only due to the presence of AC, the contribution of AC in the sorption capacity of the composite could be calculated to be 23 mg of DEA per gram of AC. As a result, AC lost an important fraction of its sorption

Table I. Sorption Constants for Composite and Chitosan Hydrogels and Activated Carbon Powder

	Activated carbon	Chitosan hydrogel	Composite hydrogel
Experimental Q_e (mg g^{-1})	280	46	49
Initial sorption kinetic coefficient			
γ (L mg^{-1} min^{-1})	3.33 10^{-5}	5.00 10^{-7}	1.67 10^{-6}
Lagergren first-order model			
k_l (h^{-1})	1.425	0.070	0.183
Calculated q_{el} (mg g^{-1})	135.7	45.4	45.8
R^2	0.963	0.965	0.978
Pseudo-second-order model			
k_{ll} [g (mg h)$^{-1}$]	0.506	0.007	0.009
Calculated q_{ell} (mg g^{-1})	381.7	28.01	45.45
R^2	0.999	0.967	0.995

capacity once embedded into the chitosan network. As shown by Figure 6(c), some AC adsorption sites were entrapped and covered by chitosan chains and as a consequence, were no longer available to adsorb DEA molecules. However, despite the incorporation of AC into the hydrogel does not significantly increase the sorption capacity, it leads to an improvement of the sorption kinetics. Table I shows an increase of the initial sorption kinetic coefficient γ from 5.00 10^{-7} L mg^{-1} min^{-1} for chitosan gels to 16.7 10^{-7} L mg^{-1} min^{-1} for composite materials, the total weight of material being the same [Figure 6(b)]. By the same way, the comparison of first order Lagergren constants (for which the agreement between calculated q_e and experimental Q_e values is more accurate than the pseudo second-order model) shows an improvement of the same order, from $k_1 = 0.070$ h^{-1} for chitosan gels to $k_1 = 0.183$ h^{-1} for composite materials. Moreover, as shown in Figure 6(a), the time needed to reach half of the sorption capacity is 4 h in the case of the composite gel when compared with 12 h for the chitosan hydrogel. Considering that the molecular diffusion of DEA through water inside the polymeric gel is not a limiting factor for sorption, the presence of AC adsorption sites clearly reduced the time required to reach the sorption equilibrium.

CONCLUSION

Chitosan and composite chitosan/active carbon hydrogels were elaborated using two different procedures: immersion in ammonia solution and exposure to ammonia vapors. The influence of both the elaboration route and the chitosan concentration was evaluated using a convergent approach involving a structural characterization and the determination of the different materials functional properties.

A similar global asymmetric morphology was obtained whatever the operating conditions, constituted by a dense layer over a macroporous sublayer. Microscopic observations and WAXS measurements contributed to highlight a slight influence of the gelation route and the chitosan concentration on the porosity of the sublayer. These micro- and nano-structural changes were correlated with mechanical properties and ESR (whose values were in agreement with those reported in published reports for a similar application). The inclusion of active carbon in the polymer matrix did not significantly affect the morphology of hydrogels or their mechanical properties. Despite the equilibrium sorption of DEA was similar for the composite and chitosan hydrogels due to the entrapment of AC particles within the polymer matrix, the addition of AC into chitosan hydrogel contributed to speed up the sorption kinetics by a factor 3, and could thus be used to adapt the kinetics of malodorous compound emissions during wound healing. It can be envisaged to adapt the AC mass ratio in the chitosan hydrogel to the healing stage of the wound. The results reported in this study indicate that these novel composite chitosan/AC hydrogels, in the form of either native hydrogels or re-hydrated lyophilizates, represent promising wound dressings for malodorous wounds. On-going studies concern the evaluation of the biological properties of the elaborated materials by means of *in vitro* and *in vivo* experiments.

ACKNOWLEDGMENTS

The authors would like to address acknowledgments to the French National Agency of Research (ANR), which supports this study through the project PANSKIT (ANR-08-MAPR-0021-01), and the BM2-D2AM staff for scattering experiments at ESRF.

REFERENCES

1. Zhou, H. Y.; Chen, X. G.; Kong, M.; Liu, C. S.; Cha, D. S.; Kennedy, J. F. *Carbohydr. Polym.* **2008,** *73*, 265.
2. Jayakumar, R.; Prabaharan, M.; Sudheesh Kumar, P. T.; Nair, S. V.; Tamura, H. *Carbohydr. Polym.* **2011,** *29*, 322.
3. Brown, M. A.; Daya, M. R.; Worley, J. A. *J. Emerg. Med.* **2009,** *37*, 1.
4. Qin, Y. *J. Appl. Polym. Sci.* **2008,** *107*, 993.
5. Saarai, A.; Sedlacek, T.; Kasparkova, V.; Kitano, T.; Saha, P. *J. Appl. Polym. Sci.* **2012,** DOI 10.1002/app.
6. Hurler, J.; Engesland, A.; Poorahmary Kermany, B.; Skalko-Basnet, N. *J. Appl. Polym. Sci.* **2012,** *125*, 180.
7. Boucard, N.; Vitona, C.; Agayb, D.; Maric, E.; Rogerc, T.; Chancerelleb, Y.; Domard, A. *Biomaterials* **2007,** *28*, 3478.
8. Ribeiro, M. P.; Espiga, A.; Silva, D.; Baptista, P.; Henriques, J.; Ferreira, C.; Silva, J. C.; Borges, J. P.; Pires, E.; Chaves, P.; Correia, I. *J. Wound Repair Regeneration* **2009,** *17*, 817.
9. Thomas, S.; Fisher, B.; Fram, P.; Waring, M. *J. Wound Care* **1998,** *7*, 246.
10. Kose, A. A.; Karabagli, Y.; Kurkçuoglu, M.; Çetin, C. *Wounds* **2005,** *17*, 114.
11. Montembault, A.; Viton, C.; Domard, A. *Biomaterials* **2005,** *26*, 1633.
12. Rivas-Araiza, R.; Alcouffe, P.; Rochas, C.; Montemlbaut, A.; David, L. *Langmuir* **2010,** *26*, 17495.
13. Venault, A.; Vachoud, L.; Bouyer, D.; Pochat-Bohatier, C.; Faur, C. *J. Appl. Polym. Sci.* **2011,** *120*, 808.
14. Venault, A.; Bouyer, D.; Pochat-Bohatier, C.; Vachoud, L.; Faur, C. *AIChE J.* **2011,** DOI 10.1002/aic.
15. Hirai, A.; Odani, H.; Nakajima, A. *Polym. Bull.* **1991,** *26*, 87.
16. Lagergren, S. K. *Sven. Vetenskapsakad. Handl.* **1898,** *24*, 1.
17. Ho, Y.S.; McKay, G. *Process Biochem.* **1999,** *34*, 451.
18. Liu, C.; Xia, Z.; Czernuszka, J.T. *Chem. Eng. Res. Design* **2007,** *85*, 1051.
19. Chang, Y.; Xiao, L.; Tang, Q. *J. Appl. Polym. Sci.* **2009,** *113*, 400.
20. Dang, Q. F.; Yan, J. Q.; Li, J. J.; Cheng, X. J.; Liu, C. S.; Chen, X. G. *Carbohydr. Polym.* **2011,** *83*, 171.
21. Head-Gordon, T.; Johnson, M. E. *Proc. Natl. Acad. Sci. USA* **2006,** *103*, 7973.
22. Li, Q.; Yang, D.; Ma, G.; Xu, Q.; Chen, X.; Lu, F.; Nie, J. *Int. J. Biol. Mol.* **2009,** *4*, 121.
23. Vachoud, L.; Pochat-Bohatier, C.; Chakrabandhu, Y.; Bouyer, D.; David, L. *Int. J. Biol. Macromol.* **2012,** *51*, 431.

24. Agulhon, P.; Robitzer, M.; David, L.; Quignard, F. *Biomacromolecules* **2012,** *13*, 215.
25. Mi, F.-L.; Wu, Y.-B.; Shyu, S.-S.; Chao, A.-C.; Lai, J.-Y.; Su, C.-C. *J. Membr. Sci.* **2003,** *212*, 237.
26. Khalid, M. N.; Agnely, F.; Yagoubi, N.; Grossiord, J. L.; Couarraze, G. *Eur. J. Pharm. Sci.* **2002,** *15*, 425.
27. Tsao, C. T.; Chang, C. H.; Lin, Y. Y.; Wu, M. F.; Wang, J. L.; Young, T. H.; Han, J. L.; Hsieh, K. H. *Carbohydr. Polym.* **2011,** *84*, 812.
28. Janvikul, W.; Thavornyutikarn, B. *J. Appl. Polym. Sci.* **2003,** *90*, 4016.
29. Ross-Murphy, S. B. In Polymer gels. Fundamentals and biomedical applications, DeRossi, D., Kajiwara, K., Osada, Y., Yamauchi, A., Eds.; Plenum Press: New-York, **1991;** p 21.
30. Zhao, L.; Luo, F.; Zhai, M.; Mitomo, H.; Yoshii, F. *Radiat. Phys. Chem.* **2008,** *77*, 622.
31. Czechowska-Biskup, R.; Rokita, B.; Lotfy, S.; Ulanski, P.; Rosiak, J. M.; *Carbohydr. Polym.* **2005,** *60*, 175.